COMPLEX STUDY OF PLASMA HOT MACHINING (PMP)

Liliana Popa
University POLITEHNICA of Bucharest, lilipopa@yahoo.com

ABSTRACT: The paper aims to provide a systemic view all phenomena accompanying assisted machining plasma (PMP). Their knowledge is imperative because it can reduce processing costs, reduces wear of cutting tools to increase productivity and processing. Addressing systemic issues provides an overview of the phenomenological complexity of the machining system with plasma jet and help to highlight new research directions in this field. Analysis of thermal fields that develop in the cutting, structural changes induced thermal fields generated by the cutting forces are carried to the processing of various types of steels, covering the scope of the heating process conducted by the plasma jet, and the phenomenology of the classic cutting with all its features.
KEY WORDS: plasma generator, plasmagen gas, thermal field, metallographic structure, cutting forces.

1. INTRODUCTION

At first glance, plasma machining features (PMP) induce believe that using this process in machining operations and especially in turning operations, are: a rational method of processing under certain conditions, one possible method, but irrational, an irrational way.
In fact, choosing the right can only be obtained after the answers to two basic questions: what we expect from XXI century materials and processing are some phenomena that produce spectacular effects for plasma machining process. For the first question, the answers are given immediately below, and analysis "in full" the phenomenology will be subject of this paper.
Trends reported in cutting refer to:
- maximum productivity with optimal machining parameters (cutting speed, feed, depth of cut);
- processes which allow for roughing and finishing processing and high speed;
- opportunities and facilities for processing materials with hardness to 65 HRC;
- processing with increased flexibility of parts with different surfaces or different types of machines;
- cost of processing flexibility in these conditions;
- minimum cost of ancillary equipment expenses.
Even these trends only selected from many others, it can be concluded that the most significant progress is achieved, both in the way of equipment and use of machine tools, but also classical and unconventional combination of processing parameters.

2. STUDY OF INFLUENCE FACTORS ON THE HOT MACHINING PLASMA

To achieve a comprehensive analysis of plasma machining (PMP) is necessary to highlight the complex system of processing, the heat brought by the jet plasma processing of materials difficult to cut Fig.1.
Establishing the interdependence of classics factors and electro technological factors on PMP can be achieved only on presentation of conditions that are required to be observed in this type of processing.
Besides the shape and dimensions of the work piece to be processed, the required surface quality after PMP, new factors that distinguish plasma assisted processing of the traditional. These factors are:

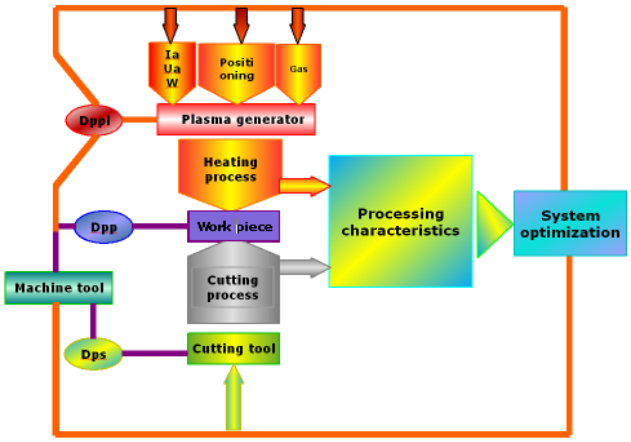

Figure 1. Technological system at PMP

- plasma generator need to locate in technological space of equipment of machine tools so we can achieve optimum handling it;
- ensure coordination between ignition time and arc fighting, on the one hand and the beginning and end of processing, on the other;
- eliminate the direct influence of plasma arc on the areas that are not processed by this method;
- avoid short circuits between the plasma generator and work piece, machine tool or tool, through the chip.
Also, the heating process, the processing by plasma assisted turning, can be efficiently than in terms of correlation with the cutting regime.
Analyzing the results obtained so far, can lay down some practical conclusions show that:
- increasing shear section on PMP, usually in terms of energy, is more advantageous than increasing the cutting speed;
- for saving additional heating energy, the more advantageous is increasing cutting regime parameters in the following order: depth of cut (t), advance (s) and cutting speed (v);
- if the depth of cut is limited, then increased the advance (s) followed by cutting speed (v).
Heat quantity introduced into the area work through the plasma jet increase temperature in the area immediately surrounding the tool, which is related to tool wear and durability, and to work piece surface, a phenomenon important for the optimization the entire process.

3. STUDY OF THERMAL PHENOMENA

Study of thermal phenomena in the area working on PMP help to establish the temperature that develops in different technological areas.

Can be distinguished so, 5 major areas, Fig. 2, which are:

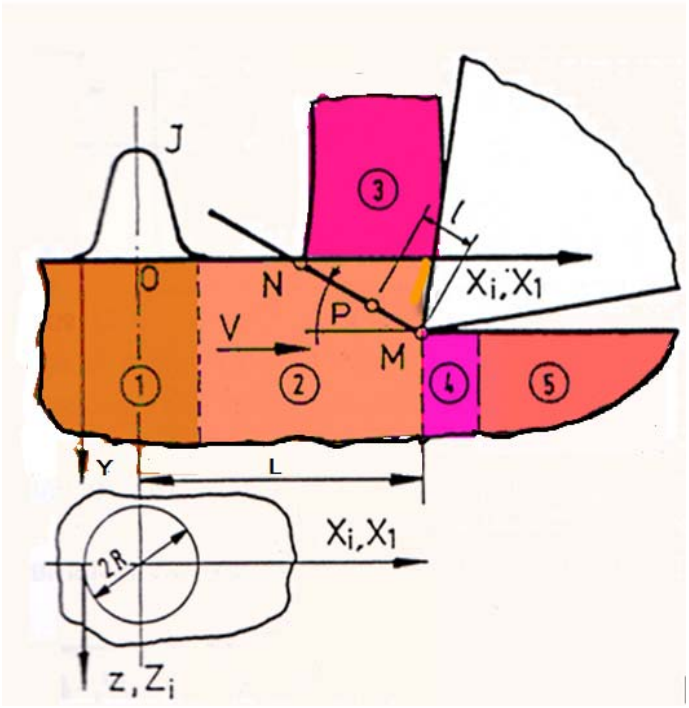

Figure 2. Thermal areas

- zone 1 - located just below the heat source (spot heating), which is characterized by the appearance of large temperature gradients in depth of material and the material softening is produced;
- zone 2 located by the edge tool, shows a temperature distribution under the laws of thermal conductivity, and heat diffusion phenomena in the environment (the area ON). It can be appreciated, however, that the equations of thermal equilibrium, the heat loss is negligible;
- zone 3 located in the chip;
- zone 4 on the surface for positioning tool represents the tool heat exchange surfaces with its clearance and settlement;
- zone 5 located outside of the cutting is of interest in terms of temperature and its influence on residual coating of the work piece material structure.

To follow the calculation of the temperature in zone 2 will start from the relation 1,[1].

$$\theta^{+} = \frac{\theta_1 \cdot l_1^{+} + \theta_2 \cdot l_2^{+}}{l_1^{+} + l_2^{+}}, \qquad (1)$$

showing the correlation between surface temperatures developed on departure, θ_1[°C] and settlement θ_2[°C] surface of the tool and contact lengths in the same area, l_1^{+} [mm], l_2^{+} [mm].

The calculation for θ_1 and θ_2 results from the basic laws of thermo physical cutting processes [6, 7]:

$$\theta_1 = \theta_F + 0{,}142 \cdot \frac{\sqrt{\omega}}{\lambda} \cdot \frac{k_\varepsilon^{+} \cdot l_1^{+}}{\sqrt{v}} \cdot (q_{1t}^{+} - 1{,}3 \cdot q_1^{+}) \qquad (2)$$

$$\theta_2 = \theta_F \cdot T_i + 0{,}1 \cdot \frac{\sqrt{\omega \cdot l_2^{+}}}{\lambda \cdot \sqrt{v}} \cdot (q_{2t}^{+} - 1{,}82 \cdot q_2^{+}) \qquad (3)$$

It established that temperatures determined by relations (2) and (3) are dependent on the material characteristics λ [W/cm· °C], ω [cm^2/s], the rate of contraction of the chip k_ε^{+} and speed cutting v [m/min], and the temperature θ_F [° C], developed in the plane of shear (sliding) of the chip. Also, the relationship between density heat flow, c_1^{+} [W/m^2] and q_2^{+} [W/m^2]. These quantities (q_1^{+} and q_2^{+}) is the result of interaction of all heat flows acting on the contact surfaces of the tool. Variable T_i [°C], indicates the temperature variation of forming heat generated penetrates the work piece.

Heat flow densities generated by the phenomenon of friction on the departure and settlement surface (q_{1t}^{+} and q_{1t}^{+}) is calculated with relations:

$$q_{1t}^{+} = 2{,}5 \cdot \frac{v(P_{zb}^{+} \cdot \sin\gamma + P_{Nb}^{+} \cdot \cos\gamma)}{b \cdot l_1^{+} \cdot k_\varepsilon^{+}} \qquad 4$$

$$q_{1t}^{+} = 3{,}25 \cdot \frac{F_2^{+} \cdot v}{b \cdot l_2^{+}} \qquad 5$$

Quantities P_{zb}^{+} and P_{Nb}^{+} represents components of cutting force P_z^{+}[N].

Since the θ_F term in relations 2 and 3 represents the temperature at the chip level sliding plane, considered to be approximately constant and equal to:

$$\theta_F \approx \theta_n + \theta_d^{+} \qquad 6$$

Temperature (θ_d^{+}) of deformation corresponding edge cutting, is calculated with:

$$\theta_d^{+} = 0{,}98 \cdot \frac{\omega}{\lambda} \cdot b_n^{*} \cdot \frac{\sin\Phi}{a \cdot b} \cdot [P_{zb}^{+} \cdot (k_\varepsilon^{+} - \sin\gamma) \cdot P_{Nb}^{+} \cdot \cos\gamma] \qquad 7$$

In relationship 7, in addition to the material characteristics (λ, ω), chip size (a, b), the cutting forces (P_{zb}^{+}, P_{Nb}^{+}), tool geometry (γ, departure angle of the tool), P_{e_0} - Pecle criteria, outlined and some of the heat that is released in the chip, by the relation:

$$b_n^{*} = \frac{1}{1 + 1{,}5 \cdot k_\varepsilon^{+} \cdot P_{e_0}^{-0{,}5}} \qquad 8$$

In 6 relation, the term θ_n represents medium temperature of heating the work piece on the core of the tool cutting edge. θ_n components expresses the influence of elements related to the plasma generator, installation of plasma heating, type and geometry of the chip and work piece characteristics.

$$\theta_n = \frac{50}{\sqrt{\pi}} \cdot \beta \cdot \frac{W \cdot \eta}{b \cdot \lambda \cdot L \cdot \sqrt{k}} \cdot \exp\left[-\frac{k_1}{100} \cdot a^2\right] \cdot \operatorname{erf}\left[\frac{b}{20} \cdot \sqrt{\frac{k_0 \cdot k_1}{k_0 + k_1}}\right] \qquad 9$$

After exposure methodology for determining the temperature and heat flow from the cutting zone, the PMP can draw some conclusions.

One can appreciate that increased power electric current in the arc plasma, in particular argon plasma, and with increasing heating temperature θn, decreases the heat flux density q_d^{+}, influencing the flow lamination material processed and increasing the length of the sliding surface of the chip, Fig.3,

Reduction under the same conditions (high intensity I) q_1^{+} flow

leads to lower friction coefficient of the previous root chip and reducing the size reduction affects q_{12}^{+} force acting on the seating surface of the tool.
With increasing heating temperature, the resistance of the work piece decreases, while reducing the value of cutting forces,[2].

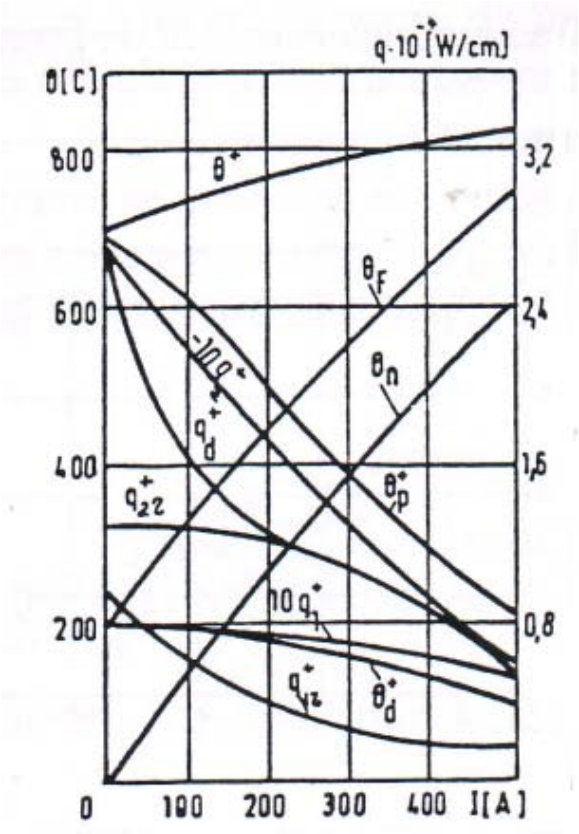

Figure 3. Variation of heat flow density

We may say that heat flows and exchanges on PMP are basically the same as in classical cutting: flow with density (q_1^{+}) is directed from chip to tool and density q_{12}^{+} is directed from tool to piece. This means that some heat in the tool within the shear plane of the work piece mass.
With increasing plasma arc power, heat transmission tool - piece drops suddenly, as part of the material coating is too warm. Reduction of q_{12}^{+} leads to strong heating of the tool.
On temperature on the contact surfaces of the tool, will hold a special importance and cutting regime.
Increase advance leads, as in classic cutting, the temperature increases θ_1 and θ_2 and thus the increases temperature cutting. Increasing the cutting speed increases the temperature θ, the classic cutting and on PMP dependence $\theta^{+}(v)$ is shown in Fig. 4.
The presence of an extreme point on the curve $\theta^{+}(v)$ is explained by classical physics processing. To increase cutting speed under a constant power of plasma arc and a distance L constant, θ_n heating temperature decreases. This leads, but, high temperature deformation θ_d^{+} in chip formation zone. Still, reduction of θ_n, as calculations show, clearly ahead of θ_d^{+} growth.
Therefore, in the absence of other factors, cutting temperature, at increase of v, would be reduced. With its reduction the cutting forces increase and total emission of heat and heat friction on the surface setting tool.

.By reducing the chip contraction coefficient (k_c^{+}), which increases the speed of sliding chip on the surface of the tool and decrease length chip contact (l_1^{+}). Is done as temperature increased friction on the tool departure surface. All these factors lead to the conclusion, already present in the graph in Fig. 4, increasing the cutting speed v leads, after an area of critical speeds, increasing the value θ^{+}.

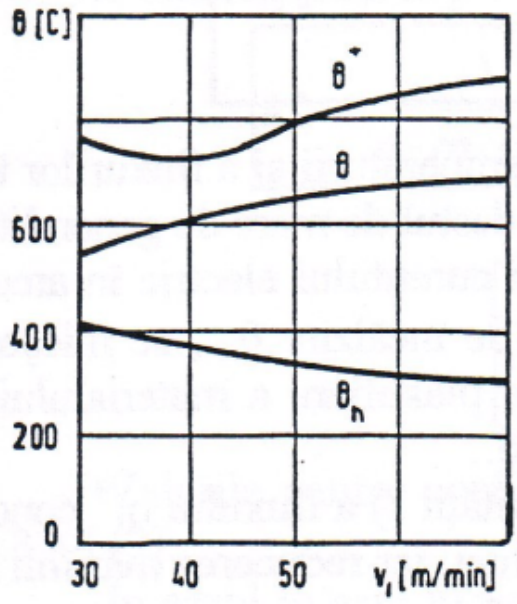

Figure 4. Cutting temperature variation depending on cutting speed [8]

4. PMP PROCESS INFLUENCE ON SUPERFICIAL COATING OF THE WORK PIECE

Temperatures that develop to PMP, above, lead to structural changes in the superficial coatings of the piece. Correlating chemical phenomena coatings with heating mechanism, depending on the type of material processed, can be issued several hypotheses for how the variation of hardness in the surface coatings.

It starts from the assumption that to heating cycle thermal plasma has the same allure with the heating CMF (with medium frequency currents) or laser heating, Fig. 5, [5].

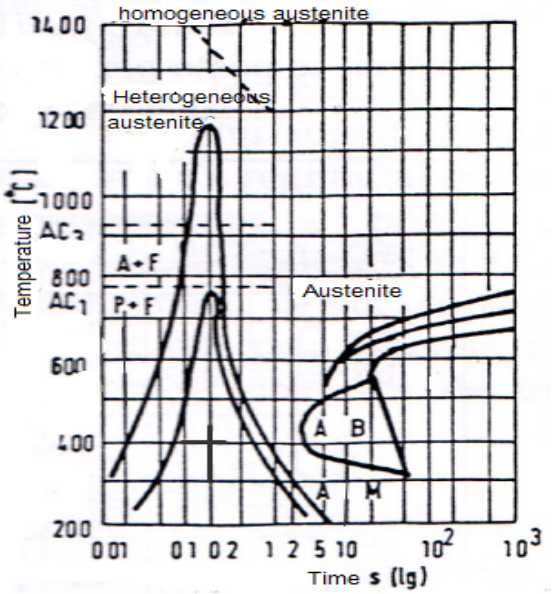

Figure 5. Thermal cycling at heating laser [5]

PMP warming, coating of the parts can reach temperatures up to the point Ac3, followed by rapid cooling, resulting in the formation zone of hardening martensitic structure, the interior retains the original structure of the material unaffected by heating. The inter coating located between the surface and heating the remaining volume of the product is done at temperatures between Ac_1 and Ac_3, forming incomplete hardening by cooling structures, with hardness values ranging from martensite corresponding to the initial structure of the material unaffected areas.

Knowing the temperature which determines the structure of hardening is important for continuity of structure and its mechanical properties.

To be linked (in structure and mechanical properties) between coats, the hardness variation curve must have a certain shape (curve 1, Fig. 6 [9]); a very sharp failure in hardness martensitic structure at the structure initial (curve 2, figure 6) promotes exfoliation of the superficial coat under the action of tensile stress or compression of the action of compressive forces; too slow a decrease of hardness (curve 3, Fig. 6) significantly reduces shock resistance.

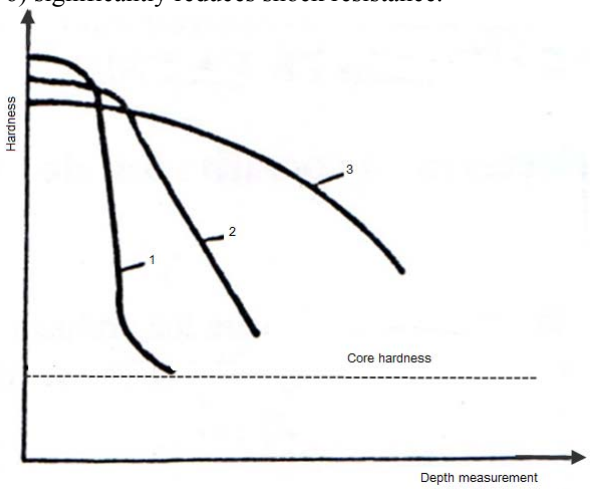

Figure 6. Variation of hardness in the surface coat depth

Another interpretation, by similarity, based on phenomena that occur at the surface directed beam hardening, leads to the conclusion that the surface layer micro hardness and depth of hardening layer structure are decisively influenced by carbon content, [9].

Hardness may increase rapidly at concentrations above 0.12% C, absolute values are influenced by working parameters (plasma power generator, heating duration, speed, etc.). Microstructure hardening coat structure could be formed martensite, ferrite (hipoeutectoide steels), residual austenite, possibly un dissolved cementite (hipereutectoide steels). The transition zone can be seen troostite or martensite recovery.

Experimental results show the existence made in the surface coats of samples made of alloy steel (34MoCN15, 19CN35 - EN 10083-1,2, C120 - EN ISO 4957), the structure of quench with martensite and bainit. There is a gradual increase of martensite content with increasing current intensity processing. Samples were taken from areas A, B, C (Fig.7).

Increasing depth of hardening zone structure is caused, in particular, by moving of critical points higher (Ac3) down, depending on the initial state and the work piece.

An application of this latter influence can provide different at structure and thermal conductivity with interphase surface ferrite / cementite different. The two phases of the mixture have very different thermal conductivities ($\lambda_{Fe3C} \approx 7$ [W / m.grd] $\lambda_{Fe} \approx 74$ W / m.grd), so that at finely dispersed mixtures (with high hardness), heat is easily dissipated in depth, while at the coarse (low hardness), heat is transmitted hard and is concentrated in the superficial layers.

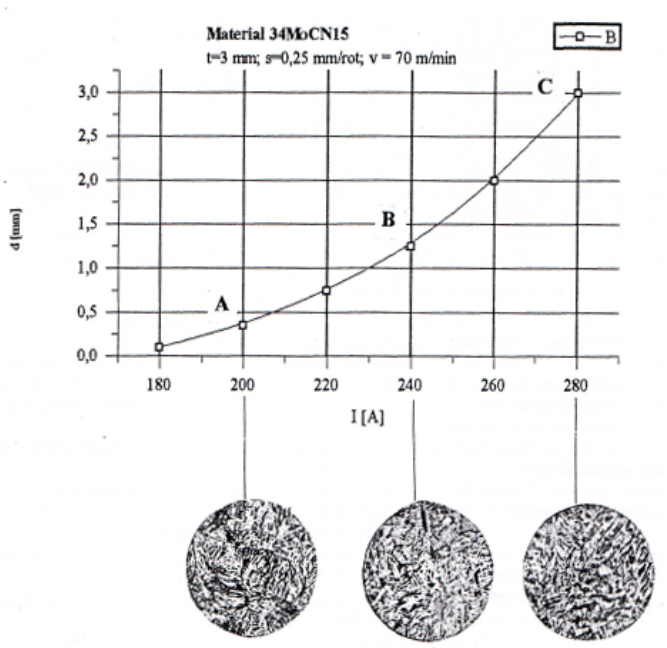

Figure 7. Thickness variation of thermal influence and types of structures depending on the current arc

Knowing formation and evolution of these structures is useful for directing the heat flow of plasma not only to improve workability, and to obtain structures with controlled hardness.

Previously presented theoretical study revealed variation of hardness in the surface coats material result by plasma-assisted processing.

To verify the hypotheses advanced, there have been several determinations for steel: 33MoC11, 34MoCN15, 20C130 and 21 TMC12.

It can be seen that the hardness was measured on metallographic samples from the inner edge, with a pitch of 0.5 mm, the measuring hardness in HRC units.

From all the data we can say that, whatever the parameter varies, the graph shows the same type of shape variations. The first area shows a low hardness, after which it increases gradually to a certain depth, and will return, finally, the initial hardness of the material, Tab.1, 2 and Fig. 8.

Following this variation is found that the maximum hardness obtained superficial layer are strongest as the arc current intensity (I) is greater and as well as feed, speed and depth of cut are smaller.

$$HRC = f\left(I, \frac{1}{s}, \frac{1}{n}, \frac{1}{t}\right) \qquad 10$$

Table.1 Hardness values in superficial layer of the piece

Depth / Nr.test	0.5	1	1.5	2	2.5	3
1	19,1	21	25	26	24	23
2	19,9	23	25	26,9	25	24
3	19,2	20	25	24	24	23,1
4	19	21	24	25,6	24,9	23
5	19,1	22	25,4	26	25	24
6	18,8	23	26,6	26	24	21
7	18,8	22	25	26,9	26	22

Table.2 Hardness values in superficial layer of the piece

Depth / Nr.test	3.5	4	4.5	5	5.5	6	7
1	20	20	20,1	20	19,8	19,5	19,1
2	21	21	20	19,5	19,6	19,2	19,2
3	22	20	20	19,6	19,3	19,1	19,2
4	21	21	20	19,5	19,2	19	19,1
5	22	20	19,1	19,5	19,2	19	19
6	19,5	19	19	19	19	19	19
7	21	19	19	19	19	19	19

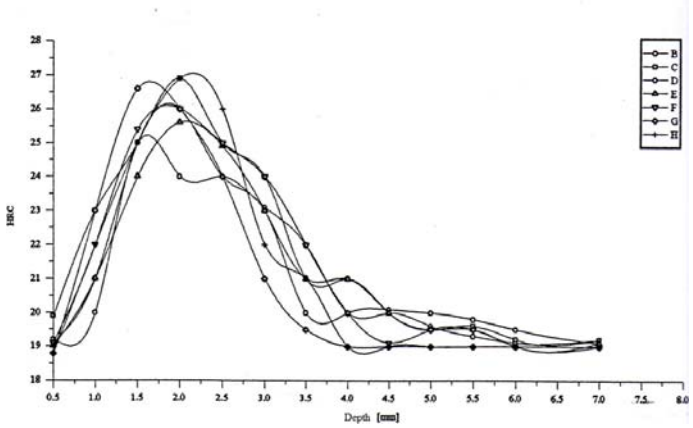

Figure 8. Variation of hardness for 34MoCN15 steel

Analyzing the obtained hardness in the superficial layer and comparing data with those in the literature [5] we can say that the values obtained correspond to a warming in the 750 to 850 ° C, and duration curves is typical of a process of heating followed by cooling without maintaining at a certain temperature.

We analyzed a chromium stainless steel, type 20C130 and heat affected coat thickness was studied. The values obtained are presented in Table 3, and the variation the function t(T) is shown in Fig. 9.

Table 3. Depth of layer heat affected in steel 20C130

I [A]	140	160	200	240	260	280	300
Depth [mm]	0,2	0,8	1,6	2,3	2,5	3,0	4

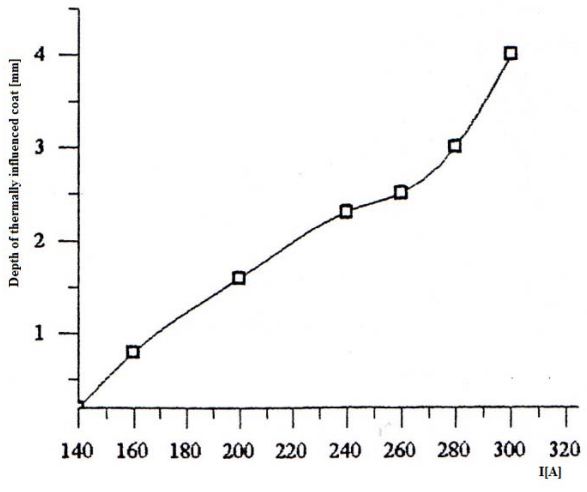

Fi

gure 9. Variation of function t(T)

Variation of hardness OF heat affected coating material is shown in Table 4 and Figure 10. It reveal the same types of variations as the steels studied previously, except that the return to baseline of hardness is achieved faster in the case of 20C130 steel.

Table 4. Hardness values in superficial coat at 20C130 steel

Depth / I[A]	0,5	1,5	2,5	3,5	4,5	5,5	Ext.
I =140 A	25	28	28	28	28	28	25
I = 160 A	25	30	28	28	28	28	25
I = 200 A	26	31	28	28	28	28	25
I = 240 A	25	31	28,5	28	28	28	25
I = 260 A	25	30	29	28	28	28	24,5
I = 280 A	26	34	29	28	28	28	24,5
I = 300 A	26	32	34	30	28	28	24

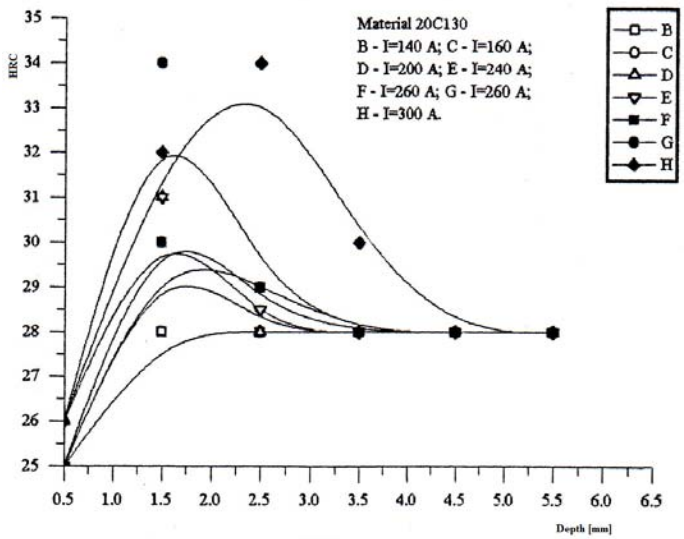

Figure 10. Variation function HRC (h)

Values for hardness material in the superficial coat corresponding to a hardening treatment, heating to 1050 ° C, followed by a return to rapid heating (V_{heat} = 100 deg / min) in the range 700 to 800 ° C. Thermally influenced layer structure is shown in Fig.11.

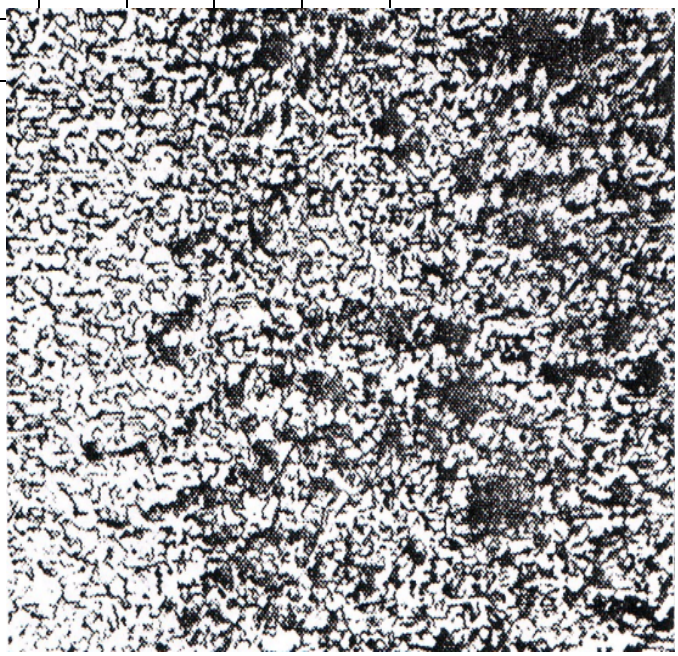

Figure 11. Coating thermally influenced for 20C130

5. FORCE STUDIES ON PMP

Study of cutting forces on PMP is another element that proves the complexity of the phenomena that accompany machining plasma, [3,4]. The size of the forces which arise from machining with plasma is related to structural changes that occur under the influence of temperature induced by plasma jet. In view of that observation, it was considered to be necessary to choose a variety of materials with different composition.

Materials used are steel for improvement (34MoCN15), alloy steel bearing (19CN35) and stainless steels (C120). Chemical composition will be presented below in Table 4-6.

Table 4. Chemical composition of steel 34MoCN15

Chemical composition, [%]							
C	Mn	Si	Cr	Ni	Mo	P_{max}	S_{max}
0,16-0,22	0,30-0,60	0,17-0,37	1,4-1,7	1,4-1,7	0,15-0,30	0,035	0,035

Table 5. Chemical composition of steel 19CN35

Chemical composition, [%]							
C	Mn	Si	Cr	Ni	Mo	P_{max}	S_{max}
0,30-0,38	0,40-0,70	0,17-0,37	1,25-1,65	3,25-3,65	-	0,035	0,035

Table 6. Chemical composition of steel C120

Chemical composition, [%]							
C	Mn	Si	Cr	Ni	Mo	P_{max}	S_{max}
1.80-2,20	0,15-0,45	0,15-0,35	12,0-14,0	max.0,35	-	0,030	0,025

Data presented in this section are taken from the literature [5] and are useful for interpreting the results of experimental research.

Ranges of independent variables that influence the process are presented below.

The current arc intensity (I) was varied between 140-260 A. It was noted that at current intensities below 140 A, arc plasma is not stable and therefore this value was considered as a lower limit. Did not use values greater than 260 A because, above this limit, appear the phenomenon of melting the metal surface. Drops of molten metal are designed after the tool, leading to damage surface finish.

Depth of cut (t), was varied between 2 and 6 mm radius. Not worked with depths of cut less than 2 mm is justified in terms of productivity. At depths of cut greater than 6 mm, there is a pronounced increase in cutting forces. Relatively low stiffness of the lathe on which experiments have been carried on lead to vibration, leading to break plates chipping and to obtain improper surfaces in terms of roughness.

Variation of advance for cutting was performed between the limits from 0.12 to 0.63 mm/rev. Were not exceeded this range for the same reasons presented in depth of cut.

Cutting speed (v), was varied within the limits allowed by the machine tool and cutting process stability. It was considered that the values can be chosen to cover a range for acceptable regimens commonly used in industry.

The force for materials processing functions indicated above, are presented in Table 7.

Table 7. Working forces to PMP

34MoCN15	19CN35	C120
$F_z = e^{\frac{e^{6.985}\cdot s^{0.725}\cdot t^{0.886}}{v^{0.164}\cdot I^{0.242}}}$	$F_z = e^{\frac{e^{6.901}\cdot s^{0.703}\cdot t^{0.934}}{v^{0.261}\cdot I^{0.242}}}$	$F_z = e^{\frac{e^{7.268}\cdot s^{0.741}\cdot t^{0.997}}{v^{0.134}\cdot I^{0.329}}}$

Spatial graphics presented, indicate the simultaneous influence of a classic parameter and the current intensity work and offers interesting information, Fig.12-14.

Thus, they emphasize the existence of a period at the beginning of the process when the variation of forces is very small. Area is dispose near the axes (with a nearly asymptotic to the axis configuration).

It can be appreciated that this change corresponds to the beginning of time until starting material plasticization, and the system enters the normal work.

Graphics also provides information on the speed of change of force in relation to two parameters. Thus, the rate of change in the intensity of current is less than that depending on the classic parameter s or t.

A special reaction in this regard, the study shows the function Fz (v, I), where, due to cumulative force reduction, speed variation as the two axes are significantly higher.

For example, below, will present the cutting force variation for steel C120, the working conditions listed in Table 8.

Table 8. Areas of variation of the cutting regime parameters for C120 steel

Nr. crt.	Code	Working system parameters				Nr.fig.
		s [mm/rev]	t [mm]	v [m/min]	I [A]	
1	Fz(s, I)	s	2,5	50	I	8
2	Fz(t, I)	0,28	t	50	I	9
3	Fz(v, I)	0,28	2,5	v	I	10

Analyzing only the influence of current intensity in plasma jet, we observe a decrease of cutting force, but not higher, Figure 15. The spectacular force reduction is achieved by accumulating heat introduced by plasma arc and the heat developing in the classic cutting.

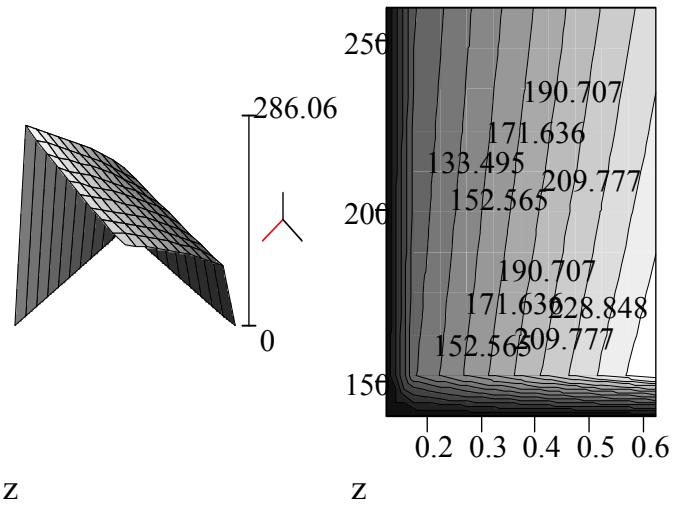

Figure 12. Variation of function $Fz(s, I)_{C120}$

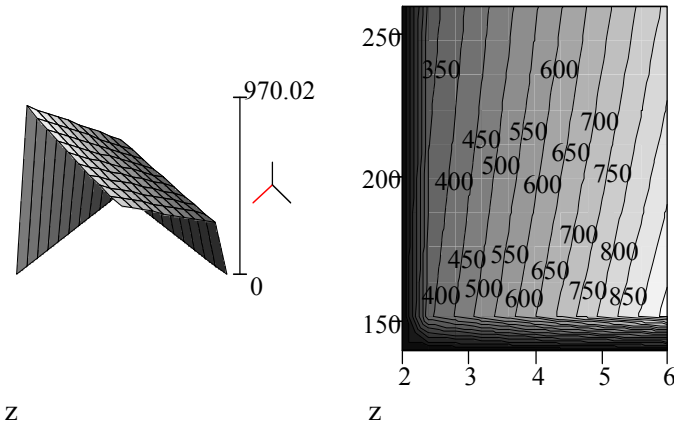

Figure 13. Variation of function $Fz(t, I)_{C120}$

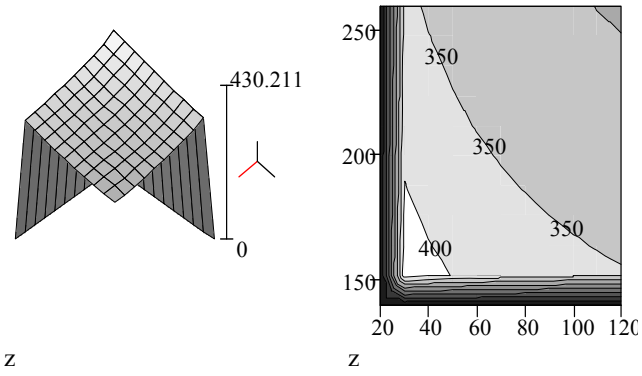

Figure 14. Variation of function $Fz(v, I)_{C120}$

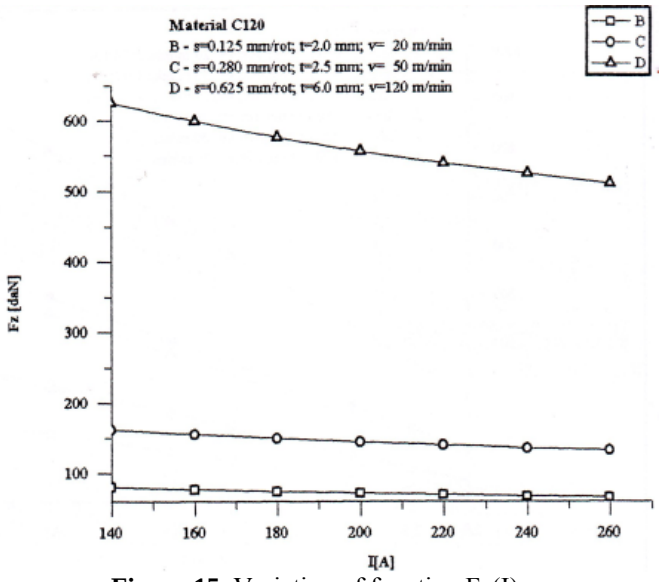

Figure 15. Variation of function $Fz(I)_{C120}$

To draw conclusions on the factors that influence the size of the cutting force at PMP will present the following data: the calculated values of cutting force in cutting classic, the calculated values of cutting force in assisted processing and values of cutting force reduction coefficient ®. Illustrations will be only for the advance variation (classical and assisted processing) and current intensity (assisted processing), Table 9.

Table 9. Values of cutting forces and the force reduction factor (R)

Nr. crt.	Function	Cutting regime	Variable	PMP force	Classical force	R [%]
1	$Fz(s)_{C120}$	t=6 mm; v=120 m/min; I=260 A	s = 0,125	154,86	262,2	40,9
			s = 0.175	198,71	337,5	41,1
			s = 0.225	239,38	407,5	41,3
			s = 0,275	277,76	473,7	41,4
			s = 0,325	314,36	536,9	41,4
			s = 0,375	349,53	597,7	41,5
			s = 0,425	383,50	656,6	41,6
			s = 0,475	416,45	713,7	41,6
			s = 0,525	448,50	769,3	41,7
			s = 0,575	479,78	823,6	41,7
			s = 0,625	510,36	876,8	41,8
2	Fz(s) 19CN35	t=6 mm; v=120 m/min; I=260 A	s = 0,125	147,77	277,4	46,7
			s = 0.175	187,20	357,1	47,6
			s = 0,225	223,37	431,1	48,2
			s = 0,275	257,22	501,1	48,7
			s = 0,325	289,27	568,0	49,1
			s = 0,375	319,89	632,4	49,4
			s = 0,425	349,31	694,6	49,7
			s = 0,475	377,72	755,0	50,1
			s = 0,525	405,25	813,9	50,2
			s = 0,575	432,02	871,4	50,4
			s = 0,625	458,10	927,6	50,6
3	Fz(s) 34MoCN15	t=6 mm; v=120 m/min; I=260 A	s = 0,125	138,94	245,2	43,3
			s = 0,175	177,33	315,6	43,8
			s = 0,225	212,77	381,1	44,2
			s = 0,275	246,09	443,0	44,5
			s = 0,325	277,77	502,1	44,7
			s = 0,375	308,14	559,0	44,9
			s = 0,425	337,41	614,1	45,1
			s = 0,475	365,74	667,5	45,2
			s = 0,525	393,27	719,5	45,3
			s = 0,575	420,08	770,3	45,5
			s = 0,625	446,26	820,0	45,6

Graphs for these variations are present in the figures 16 to 18.
Based on information provided by variation for processing force functions in relation to various parameters of the cutting regime can make a comparative study to exploit the influence of chemical composition, mechanical properties and metallographic structure on size of principal cutting force (Fz) on PMP.
Analyzing the influence of chemical composition of material shows that steels have an alloying element (C120), two alloying elements (19CN35) and three alloying elements (34MoCN15).
It can be appreciated [9] that chromium, nickel along is part of the alloying elements which have a crystal lattice and a value similar to the atomic radius of iron γ, which means that it would not significantly affect the cutting process. When the content of alloying elements increases, form compounds as carbides, which worsen working conditions.
Molybdenum contribute to decrease machinability steel, which can be explained by differences that exist between the lattice type and value of atomic radius of molybdenum and iron α. Depending on the structure obtained at cooling air, steel C120 is part of the steels that form double carbide , steel 19CN35 is on the border of pearlitic and martensitic steels and 34MoCN15 is part of pearlitic steels.

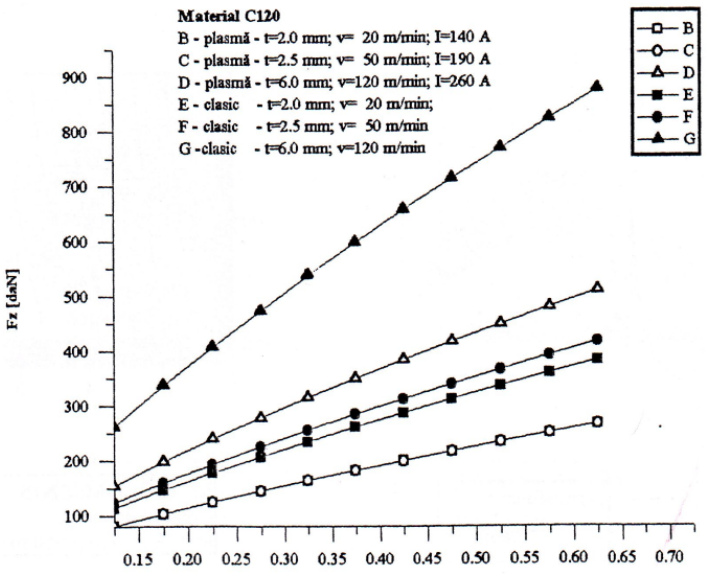

Figure 16. Variation of function $Fz(s)_{C120}$

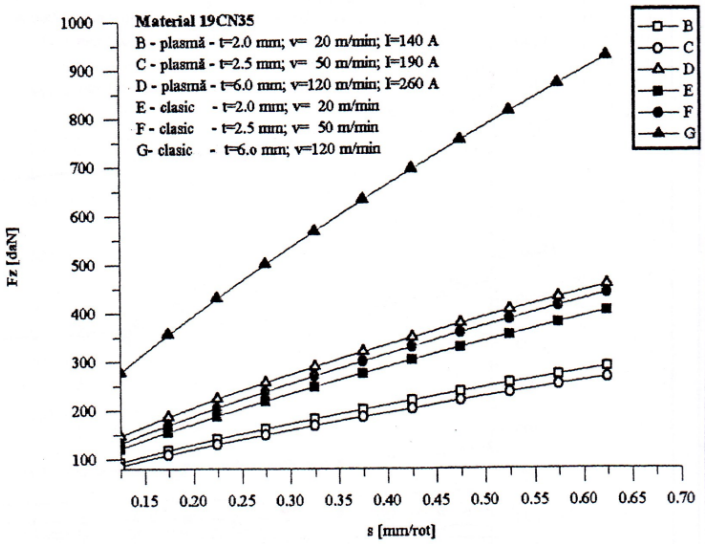

Figure 17. Variation of function $Fz(s)_{19CN35}$

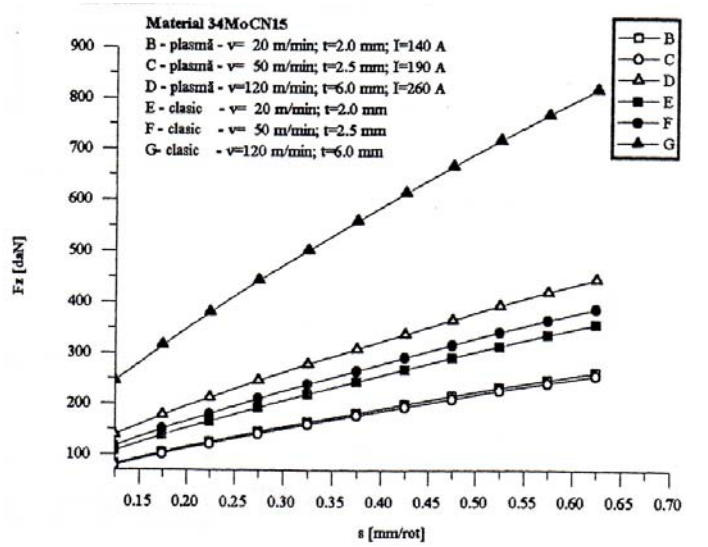

Figure 18. Variation of function Fz(s)

The literature [9] estimates that the cutting forces are lower in normal constituents (ferrite, pearlite, carbide secondary). They take usually high values for structural constituents for quenching and tempering (sorbite, martensite, globular pearlite).

The cutting forces measured and calculated at PMP confirmed same principles of variation. Thus, the forces recorded at C120 and 19CN35 steels and are higher than in steel 34MoCN15.

Influence of cutting regime on the level of cutting forces result in reduced force coefficient values (R).

Almost constant values (or slight variations) of the coefficient of reduction of cutting force at in a machining system at the minimum values of the independent process variables (s, t, v) can be explained by the fact that the reduction of strength material is determined largely by the heat introduced by plasma jet and less influence normally heat released during the cutting process. Regimes more intense work, the influence of heat generated by cutting the piece makes the induced temperature increase, the result being a greater reduction in cutting forces. For these schemes the reduction factor increases by 13 percent.

6. CONCLUSIONS

Theoretical considerations and experimental results contained in this paper lead to the formulation of the advantages of mechanical application of plasma processing of materials of future: reduction of tensile in material processed approx. 60-70%; possibility of processing parts with hardness until to 50-60 HRC; achieve a productivity of 10 to 15 times higher than for cutting cold; reduce by 40-50% the size of the cutting forces compared to conventional cutting; hardness of the surface coat obtained after processing eliminates, in some cases subsequent thermal treatment processing, or otherwise, can lead to superficial hardness machined by PMP.

7. REFERENCES

1. Ali, F., *Modélisation et simulation thermomécaniques de la coupe des métaux,* Thèse de l'Ecole Nationale Supérieure d'Arts et Métiers, Paris, (2001).
2. Battaglia, J.L., Puigsegur, L., s.o. *Méthod d'estimation de température et de flux de chaleur dans certains procédés d'usinage,* Rev. Mécanique et Industrie, 5, p. 49-60, (2004).
3. Kitagawa, T., Maekawa, K., Plasma-arc aided machining for difficult to cut materials, *Bulletin Japan Society of Precision Engineering* ,18-4 pp. 349-350, (1980)
4. Kitagawa, T., Katsuhiro, K., Kudo, A., Plasma hot machining for high hardness metals*, Bulletin Japan Society of Precision Engineering*, 22-2 (1988) p145-151
5. Popescu, N., *Unconventional heat treatments*, Editura Tehnică, Bucureşti, (1990).
6. Reznikov, A.,N., *Teplofizica rezania*, Moskva, Maşinostroenie, (1969).
7. Reznikov, A.,N., Teplofizica proţesov mehaniceskoi obrabotki materialov, *Maşinostroenia*, Moskva, (1981).
8. Reznikov, A.,N., Obrabotka metallov rezaniem s plazmerinîm nagrevom, Maşinostroeni,e Moskva, (1986).
9. Vissarion, Al,C., *Physical metallurgy and heat treatment*, Litografia Institutului de Căi Ferate, Bucharest, (1957).
10. Tosun, N., Ozler, L., *Optimisation for hot turning operations with multiple performance characteristics,* the international jourbal of Advanced Manufacturing technology, Volume 23, Nr.11-12, (2004).